Sci

MDPI

Article

Co-Processing of $[Fe(NH_2trz)_3](2ns)_2$ and UHMWPE into Materials Combining Spin Crossover and High Mechanical Strength

Manuel Baumgartner, Raphael Schaller, Paul Smith, Irene Weymuth and Walter Caseri *

Department of Materials, ETH Zürich, Vladmir-Prelog-Weg 5, 8093 Zürich, Switzerland; manuel.baumgartner@wysszurich.ch (M.B.); raphael.schaller@nolax.com (R.S.); paul.smith@mat.ethz.ch (P.S.); irene.weymuth@gmx.ch (I.W.)

* Correspondence: walter.caseri@mat.ethz.ch

Abstract: The coordination polymer $[Fe(NH_2trz)_3](2ns)_2$ (NH_2trz = 4-amino-1,2,4-triazole and $2ns^-$ = counterion 2-naphthalene sulfonate) exhibits the rare phenomenon of spin crossover in an attractive temperature range, i.e., somewhat above room temperature. Spin crossover in $[Fe(NH_2trz)_3](2ns)_2$ is manifested by thermochromism, which is accompanied by a magnetic transition from diamagnetism to paramagnetism. However, $[Fe(NH_2trz)_3](2ns)_2$ is brittle and difficult to process, which limits its use. In this study, we show that $[Fe(NH_2trz)_3](2ns)_2$ can be co-processed with ultrahigh molecular weight polyethylene (UHMWPE), which possesses outstanding mechanical properties, particularly when tensile-drawn. Therefore, $[Fe(NH_2trz)_3](2ns)_2$–UHMWPE blends were gel-processed by extrusion, employing a relatively poor solvent, which has recently been shown to offer advantages compared to good solvents. Uniform and flexible films, ribbons and fibers with $[Fe(NH_2trz)_3](2ns)_2$ fractions as high as 33.3% *m*/*m* were obtained that could be readily drawn. Spin crossover in the coordination polymer is retained in these materials, as evident from their thermochromism. The tensile strength and Young's modulus of the blends exceed those of typical commodity polymers. Thus, the films, ribbons and fibers constitute a special class of multifunctional materials that combine the flexibility and excellent mechanical properties of drawn UHMWPE with the spin crossover behavior of $[Fe(NH_2trz)_3](2ns)_2$.

Keywords: coordination polymers; spin crossover; thermochromism; polyethylene; blends; uniaxial solid-state drawing

Citation: Baumgartner, M.; Schaller, R.; Smith, P.; Weymuth, I.; Caseri, W. Co-Processing of $[Fe(NH_2trz)_3](2ns)_2$ and UHMWPE into Materials Combining Spin Crossover and High Mechanical Strength. *Sci* **2021**, *3*, 7. https://doi.org/10.3390/sci3010007

Received: 11 August 2020
Accepted: 23 December 2020
Published: 7 January 2021

1. Introduction

Coordination polymers of iron(II) and 4-amino-1,2,4-triazole (NH_2trz) (Figure 1) of the generic formula $[Fe(NH_2trz)_3]X_2$, with X a negatively charged counter ion, have attracted attention for their spin-crossover behavior [1–12]. Spin crossover is a rare phenomenon that designates a reversible change in spin state of a compound by an external trigger, for instance a change in temperature [13–19]. In the case of iron(II), a d^6 ion, spin crossover originates in a change of the low spin state with S = 0 to the high spin state with S = 2 upon increase in temperature and vice versa. That change in spin state is reflected by a transition from diamagnetic to paramagnetic behavior and also vice versa [20]. That transition from the low spin state to the high spin state is associated with a reversible color change, i.e., those compounds exhibit a thermochromic behavior [21,22]. In complexes of iron(II) and NH_2trz the low spin state typically manifests in a pink color and the high spin state in a white color [1,10,11]. Notably, the spin crossover temperature markedly depends on the counter anion X [4,23]. In this study emphasis was put on substances with spin crossover occurring somewhat above room temperature, as such compounds can potentially be used as active components in temperature-initiated switchable devices [18,24–27]. This is the case, e.g., for X = 2-naphthalene sulfonate (2ns), which has been studied extensively in solution and in the solid state [4,10–12].

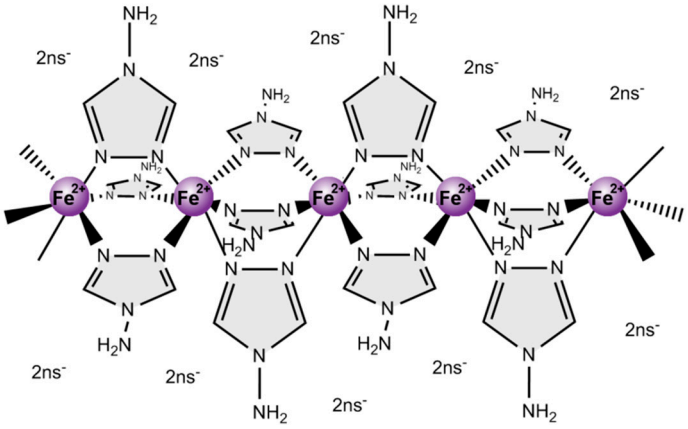

Figure 1. Schematic representation of the structure of the coordination polymer with the generic formula $[Fe(NH_2trz)_3](2ns)_2$.

There are a number of reports on the processing of spin-crossover coordination polymers, in particular $[Fe(NH_2trz)_3]X_2$, a prerequisite to obtaining materials that can be useful in technological applications. Processing of related compounds has been conducted by solution casting of iron(II) complexes with alkyl-substituted 1,2,4-triazole ligands (Rtrz) to films of the neat polymers [28,29] or of blends with poly(methyl methacrylate) [30] or polystyrene [29]. Films of $[Fe(NH_2trz)_3](2ns)_2$ were prepared from gels on glass [11] or quartz substrates [12] or from a suspension of $[Fe(NH_2trz)_3](NO_3)_2 \cdot 0.5H_2O$ in dissolved polystyrene deposited on glass [9]. Moreover, thin films of Rtrz and Htrz (1*H*-1,2,4-triazole) or NH_2trz complexes were prepared by stamping microcontact printing or spin coating, respectively [31,32]. Suspensions of nanoparticles of complexes with mixed Htrz and trz (1,2,4-triazolate) ligand sphere were also used for the deposition of thin films [32]. Patterning of spin-crossover films can be performed by lithography [31,32]. Spin crossover was observed in all those films.

Manufacture of continuous objects was achieved by their incorporation in silica monoliths prepared by a sol-gel process or by growth of spin-crossover nanoparticles in cylindrical pores of preformed silica monoliths [32,33]. There are several reports of freestanding films prepared by solution casting, such as of polymers based on vinylidene fluoride containing an iron(II) complex with Htrz, trz and NH_2trz, of poly(methyl methacrylate) or polystyrene and Rtrz complexes, of poly(oxetane) and a complex with hydroyethyl-substituted 1,2,4-triazole, and of poly(vinyl pyrrolidone) and NH_2trz complexes [32]. In addition, preformed films of Nafion can be impregnated with solutions of Htrz or NH_2trz and iron(II) ions to yield films with spin-crossover properties [32]. Further, films of natural polymers based on cellulose were impregnated with solutions of iron(II) complexes and Htrz/trz or NH_2trz ligand sphere [33]. Cellulose was also employed as the matrix for sheets of 15 mm width comprising Htrz/trz complexes [33]. Composites of polypyrrole comprising an iron(II) complex with Htrz/trz ligand sphere were obtained upon in situ polymerization of pyrrole, and the materials thus obtained were further processed to films by sintering under pressure [33]. The conductivity of those materials changed at the spin crossover temperature of the incorporated complex, which is assumed to be a consequence of the thermally induced volume change associated with the spin crossover [32]. Objects of various shapes were produced by 3D printing of a photoresist with $[Fe(NH_2trz)_3]SO_4$ [33].

Electrospinning was applied for the preparation of fibers of polystyrene with a Rtrz complex (about 3 μm fiber diameter) and of poly(lactic acid) with Htrz/trz of NH_2trz complexes [33]. Fibers consisting of a blend of a complex with Rtrz and ultrahigh-molecular-weight polyethylene (UHMWPE) were manually drawn from xylene solution and varied considerably in thickness along them [34].

Notably, the fraction of active spin crossover centers in complexes with NH_2trz ligands is strikingly higher than with Rtrz ligands [10]. On the other hand, free-standing films

or fibers of $[Fe(NH_2trz)_3](2ns)_2$ could not be obtained due to the high brittleness of this coordination polymer [11]. Therefore, blends of $[Fe(NH_2trz)_3](2ns)_2$ and UHMWPE are of particular interest since those materials might combine the outstanding mechanical properties of drawn UHMWPE and the spin-crossover behavior of $[Fe(NH_2trz)_3](2ns)_2$. For this purpose, the solution-spinning/drawing process, which came to be known as gel-spinning, appears suited as it allows the fabrication of ultrahigh-modulus and ultrahigh-strength UHMWPE fibers, ribbons and films processed from semi-dilute solutions [35,36]. Accordingly, this study explores processing of UHMWPE–$[Fe(NH_2trz)_3](2ns)_2$ blends into uniform objects such as ribbons, films and fibers, which are designed to possess extraordinary mechanical properties combined with spin-crossover behavior.

Noteworthy, processing from solution basically involves less shear-induced degradation of fillers than melt processing and thus the macromolecular $[Fe(NH_2trz)_3](2ns)_2$ is better preserved during processing of the blends. Common processing of UHMWPE (including blends) proceeds by solution-spinning into gel precursors with good solvents such as decalin (decahydronaphthalene) [35–37]. Interestingly, it was shown recently that relatively poor solvents such as stearic acid are advantageous as they lead to higher maximum draw ratios and accompanying higher Young's modulus and tensile strength at the same volume fraction of UHMWPE [38]. The maximum draw ratio increases with decreasing volume fraction of UHMWPE and reaches, e.g., a high value of 65 at an UHMWPE–stearic acid mass ratio of 1:9 [38] (N.B. since the density of UHMWPE, 0.93 g/cm^3–0.94 g/cm^3 [39], and stearic acid, 0.94 g/cm^3 [40], are similar; the mass fractions are also close to the volume fractions). Resulting UHMWPE materials were found to exhibit mechanical properties in the very high-end region of polymers, namely a tensile strength of about 3.6 GPa and a Young's modulus of about 185 GPa [38]. Accordingly, a similar procedure was adopted to prepare and study blends of $[Fe(NH_2trz)_3](2ns)_2$ and UHMWPE. In addition, employment of stearic acid permitted the formation of homogenous blends of the inherently polar $[Fe(NH_2trz)_3](2ns)_2$ and the non-polar UHMWPE, as elaborated on in the Discussion.

2. Materials and Methods

2.1. General

Ultrahigh-molecular-weight polyethylene (UHMWPE) GUR4120 (weight-average molecular weight approximately 5×10^6 g/mol) was obtained from Ticona (Sulzbach, Germany) and stearic acid from AppliChem (Darmstadt, Germany). Both substances were used as received. The coordination polymer $[Fe(NH_2trz)_3](2ns)_2$ was synthesized as described previously [10].

2.2. Processing of the Blends into Ribbons and Fibers

UHMWPE solutions were prepared with three different $[Fe(NH_2trz)_3](2ns)_2$ contents (mass ratios between UHMWPE and $[Fe(NH_2trz)_3](2ns)_2$ 10:1, 10:3 and 10:5 or 9.1% *m*/*m*, 23.1% *m*/*m* and 33.3% *m*/*m*, respectively). The mass ratio between UHMWPE and the solvent stearic acid was held constant at 1:9 in all experiments. [N.B. A formulation with a mass ratio of 10:1 between UHMWPE and $[Fe(NH_2trz)_3](2ns)_2$ consists in proportions of 1 g UHMWPE, 0.1 g $[Fe(NH_2trz)_3](2ns)_2$ and 9 g stearic acid.] The required amounts of UHMWPE, $[Fe(NH_2trz)_3](2ns)_2$ and stearic acid were added to a 25 mL round-bottomed flask. The continuously stirred mixture was heated to 80 °C for 15 min to ensure homogenization. Approximately 6 mL of slurry was collected with a syringe and fed into a laboratory recycling twin-screw micro-compounder (CPC Eindhoven, Eindhoven, The Netherlands), operating at 120 rpm under a nitrogen blanket. Processing was performed at a temperature of 160 °C; all solutions were mixed for 10 min prior to extrusion. Subsequently, the extruded ribbons were rolled to sheets of 0.7 mm thickness and were allowed to cool to room temperature.

Diethyl ether (Sigma-Aldrich, St. Louis, MO, USA) was used as extraction agent for the stearic acid. First, three extruded samples of ~$10.0 \times 100.0 \times 0.7$ mm^3 (solution-processed with a formulation of 1 g UHMWPE, 0.1 g $[Fe(NH_2trz)_3](2ns)_2$ and 9 g stearic acid) were

washed under constant stirring in ~150 mL diethyl ether in a 250 mL thread vial. After certain washing times, the samples were taken out, dried in a vacuum oven (~10 mbar) at 60 °C for ~10 min, and the mass was recorded. It was observed that after 10 min exposure to diethyl ether the stearic acid was essentially washed out of the extrudates. Thus, all extruded samples were washed for at least 10 min in diethyl ether.

For drawing, washed and dried extruded ribbons were cut to pieces with dimensions of 2 × 30 mm^2 and tensile-drawn on a Kofler bench between 100 and 130 °C to a draw ratio (λ; =ratio between final and initial sample length) of 10 and 65, respectively.

For the manufacture of fibers, a formulation of 1 g UHMWPE, 0.5 g $[Fe(NH_2trz)_3](2ns)_2$ and 9 g stearic acid was prepared as described above. Instead of washing the blends directly after extrusion, the material was pressed at 80 °C to pellets to ease feed into the syringe of a laboratory fiber-spinning-line (DACA Instruments, Santa Barbara, CA, USA). Spinning was performed at 160 °C, with an air-gap of ~1 cm between the spinneret nozzle and the quenching bath (ice water as quenching medium). The take-up speed was always maintained 10 times faster than the extrusion speed, which resulted in a draw-down ratio of ~10. The as-spun fibers were wound up on an aluminum cylinder to facilitate the subsequent washing step, also in diethyl ether under constant stirring for at least 10 min (see above).

2.3. Mechanical Properties and Thermal Analysis

A frame was made by cutting a 70 × 10 mm^2 window in a light cardstock-grade (160 g m^{-2}) paper. The films were longitudinally glued (with a two-component adhesive; Araldite® Standard) onto the frame, ensuring that variation in the initial sample length of 70 mm for tensile testing was kept to a minimum. Tensile measurements were carried out using an Instron 5864 static mechanical tester fitted with a 100 N load cell and equipped with mechanical clamps. A constant elongation rate of 20 mm min^{-1}, determined by the cross-head speed, was used throughout. All tests were performed at room temperature (~20 °C). The cross-sectional areas of the samples were calculated from their respective lengths and masses, with the latter determined using an ultra-micro balance (UMT2, Mettler Toledo, Greifensee, Switzerland), assuming a density of 1 g cm^{-3}.

Differential scanning calorimetry (DSC) was performed using a DSC 822*e* instrument (Mettler Toledo, Greifensee, Switzerland), routinely calibrated using indium standards. DSC thermograms were recorded under nitrogen flow at 10 °C min^{-1} heating and cooling rates. Samples were first heated from 25 to 60 °C and cooled to 20 °C, subsequently heated from −20 to 250 °C and cooled to −20 °C and heated again to 250 °C and finally cooled to 25 °C. The typical sample mass was ~5 mg.

3. Results

As indicated above, an UHMWPE–stearic acid mass ratio of 1:9 was applied for the preparation of homogeneous blends of UHMWPE and $[Fe(NH_2trz)_3](2ns)_2$. Homogeneous ribbons (thickness 0.7 mm) of $[Fe(NH_2trz)_3](2ns)_2$–UHMWPE blends were prepared by extrusion of the two components in stearic acid at 160 °C, i.e., well above the melting temperature of the acid (71 °C [41]). Thereafter, the stearic acid solvent was removed from the extruded ribbons by immersion in diethyl ether until the mass of the sample remained constant upon further immersion, which took about 10 min. Mass ratios between UHMWPE and $[Fe(NH_2trz)_3](2ns)_2$ of 10:1, 10:3 and 10:5 were employed, corresponding to $[Fe(NH_2trz)_3](2ns)_2$ mass fractions of 9.1%, 23.1% and 33.3%, respectively. Processing with a $[Fe(NH_2trz)_3](2ns)_2$ fraction as high as 33.3% also proceeded in a straightforward manner and resulted in flexible ribbons (cf. Figure 2); despite the high brittleness of $[Fe(NH_2trz)_3](2ns)_2$ itself.

Figure 2. Ribbon of an ultrahigh-molecular-weight polyethylene (UHMWPE)–$[Fe(NH_2trz)_3](2ns)_2$ blend comprising 33.3% *m*/*m* $[Fe(NH_2trz)_3](2ns)_2$ prepared by gel-processing with stearic acid as solvent (formulation of 10% *m*/*m* UHMWPE in 90% *m*/*m* stearic acid), after extraction of stearic acid in diethyl ether. The width of the ribbon amounts to ~10 mm (sample is undrawn).

At room temperature, the blends exhibited the typical pink color of $[Fe(NH_2trz)_3](2ns)_2$ in its low spin state. The thermochromic behavior of $[Fe(NH_2trz)_3](2ns)_2$ also occurred in the blends with the translucent UHMWPE: upon heating the color changed reversibly to white, in line with the color of the high spin complex (Figure 3), and the color transition became evident at around 40 °C, although the samples were still slightly pink at 50 °C. Eventually they become white (colorless) at around 60 °C, in agreement with thin films prepared by drying of gels of neat $[Fe(NH_2trz)_3](2ns)_2$ on glass substrates [11].

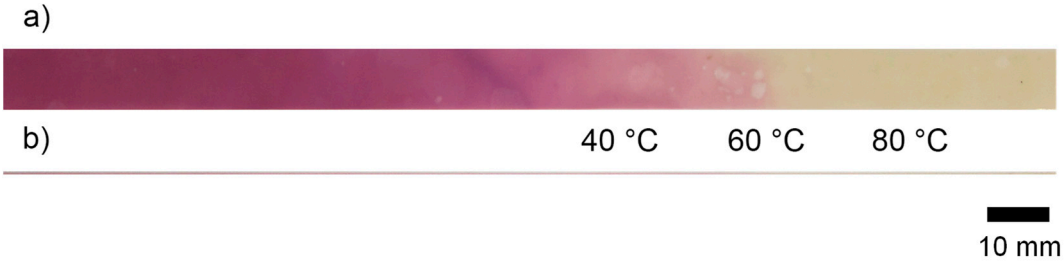

Figure 3. (**a**) Ribbon and (**b**) fiber of an UHMWPE–$[Fe(NH_2trz)_3](2ns)_2$ blend comprising 33.3% *m*/*m* $[Fe(NH_2trz_3)](2ns)_2$. The ribbon was prepared by gel-processing with stearic acid as a solvent, followed by extraction of stearic acid in diethyl ether, and the fiber by gel-spinning (see above). The samples were placed on a Kofler bench, i.e., a heating bench that features a temperature gradient.

Differential scanning calorimetry (DSC) of blends with 33.3% *m*/*m* $[Fe(NH_2trz)_3](2ns)_2$ prior to and after drawing (draw ratio 10) featured three thermally well separated endothermic peaks (Figure 4). These are attributed to different transitions, namely (at increasing peak temperature) the spin crossover of $[Fe(NH_2trz)_3](2ns)_2$, melting of UHMWPE [35] and a reversible transition at high temperature, characteristic of $[Fe(NH_2trz)_3](2ns)_2$ and due to a transition from a columnar rectangular to a columnar hexagonal packing [11] (Table 1). The spin crossover temperatures (T_{SCO}) and the reversible transition at high temperature (T_{high}) of $[Fe(NH_2trz)_3](2ns)$ are not shifted considerably upon drawing (see below) and are in the range of the values reported for the neat compound [11], as well as the melting temperature of UHMWPE [35,39]. A slight increase in the melting temperature of UHMWPE of 5 °C after drawing is common and associated with an enhanced degree of crystallinity of the polymer chains upon tensile deformation [35]. Hence, the extrusion and drawing processes did not affect the thermal transitions of $[Fe(NH_2trz)_3](2ns)_2$. In particular the spin crossover of $[Fe(NH_2trz)_3](2ns)$ is retained in blends with UHMWPE. Due to the reversibility of the transitions, the related exothermic transitions emerge also in the DSC thermograms upon

cooling; as usual due to supercooling with a hysteresis of about 20–30 °C (at heating and cooling rates of 10 °C/min).

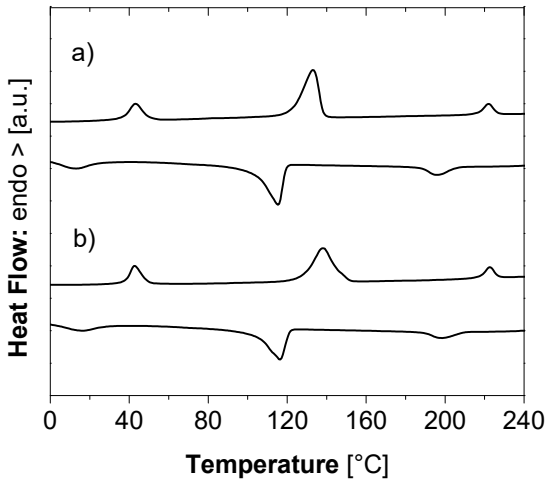

Figure 4. Differential scanning calorimetry (DSC): thermograms recorded during heating and cooling of ribbons of UHMWPE–$[Fe(NH_2trz)_3](2ns)_2$ blends comprising 33.3% *m*/*m* $[Fe(NH_2trz)_3](2ns)_2$. The ribbons were prepared by gel-processing with stearic acid as a solvent followed by extraction of stearic acid with diethyl ether. (**a**) undrawn, (**b**) drawn to a draw ratio of 10.

Table 1. Peak temperatures observed in DSC thermograms (heating/cooling cycles) of UHMWPE–$[Fe(NH_2trz_3)](2ns)_2$ blends comprising 33.3% *m*/*m* $[Fe(NH_2trz)_3](2ns)_2$ represented in Figure 4, in the undrawn state (λ = 1) and after drawing to a draw ratio λ of 10. T_{SCO} denominates the spin crossover temperature of $[Fe(NH_2trz)_3](2ns)_2$, T_m the melting temperature of UHMWPE and T_{high} a characteristic high-temperature transition of $[Fe(NH_2trz)_3](2ns)_2$.

λ [–]	T_{SCO} [°C]	T_m [°C]	T_{high} [°C]
1	43/13	133/115	222/196
10	43/16	138/116	223/199

The ribbons of neat UHMWPE and the blends comprising 9.1% *m*/*m* $[Fe(NH_2trz)_3](2ns)_2$ could readily be tensile-drawn to a draw ratio of 65, which is reported to be the maximum draw ratio of UHMWPE at the conditions applied here [38]. Accordingly, it appears that the presence of 9.1% *m*/*m* $[Fe(NH_2trz)_3](2ns)_2$ does not affect the drawing process considerably. However, with blends comprising 23.1% *m*/*m* and 33.3% *m*/*m* $[Fe(NH_2trz)_3](2ns)_2$ such high draw ratios could not be achieved; as a consequence, those samples were drawn to standard draw ratios of 10. Mechanical properties of extruded UHMWPE–$[Fe(NH_2trz)_3](2ns)_2$ ribbons (after stearic acid extraction with diethyl ether) comprising different $[Fe(NH_2trz)_3](2ns)_2$ fractions and subjected to different draw ratios are presented in Table 2. Expectedly, the Young's modulus and tensile strength are considerably influenced by the draw ratio: these values were 3–4 times higher at a draw ratio of 65 than 10 (for neat UHMWPE and blends with 9.1% *m*/*m* $[Fe(NH_2trz)_3](2ns)_2$). The samples comprising 9.1% *m*/*m* and 23.1% *m*/*m* $[Fe(NH_2trz)_3](2ns)_2$ only exhibited moderate differences in Young's modulus, tensile strength and also strain at break within the error limits. At 33.3% *m*/*m*, Young's modulus and tensile strength were significantly lower but still relatively high compared to typical commodity polymers. The strain at break of samples of a draw ratio of 10 was slightly above that at a draw ratio of 65, as commonly observed. Encouragingly, at a given draw ratio, the strain at break was not significantly influenced by the presence of $[Fe(NH_2trz)_3](2ns)_2$ at any of the fractions of the coordination polymer investigated.

Table 2. Young's modulus (E), tensile strength (σ) and strain at break (ε) of UHMWPE and UHMWPE–$[Fe(NH_2trz)_3](2ns)_2$ ribbons prepared by gel-processing from stearic acid (formulation of 10% m/m UHMWPE in 90% m/m stearic acid) at different fractions of $[Fe(NH_2trz_3)](2ns)_2$ (f) with respect to UHMWPE and different draw ratios (λ). The standard deviations are indicated in brackets.

f [% m/m]	λ [–]	E [GPa]	σ [MPa]	ε [%]
0.0	10	45 (9)	790 (25)	7 (1)
0.0	65	161 (13)	3070 (280)	3 (1)
9.1	10	33 (8)	820 (75)	7 (2)
9.1	65	145 (25)	2410 (160)	3 (1)
23.1	10	37 (2)	700 (70)	5 (1)
33.3	10	17 (6)	440 (70)	6 (2)

It was also possible to manufacture fibers of UHMWPE–$[Fe(NH_2trz)_3](2ns)_2$ blends with high content of the coordination polymer (33.3% m/m). For the preparation of such fibers, pieces of extruded strands, still containing the solvent stearic acid (see above), were pressed into pellets at 80 °C to feed the fiber spinning line. Fibers were spun at 160 °C, rolled on an aluminum cylinder and subsequently washed with diethyl ether to remove the stearic acid. The fibers were uniform (thickness 0.35 mm) and flexible. They could readily be rewound and used for, for instance, knitting fabrics (Figure 5).

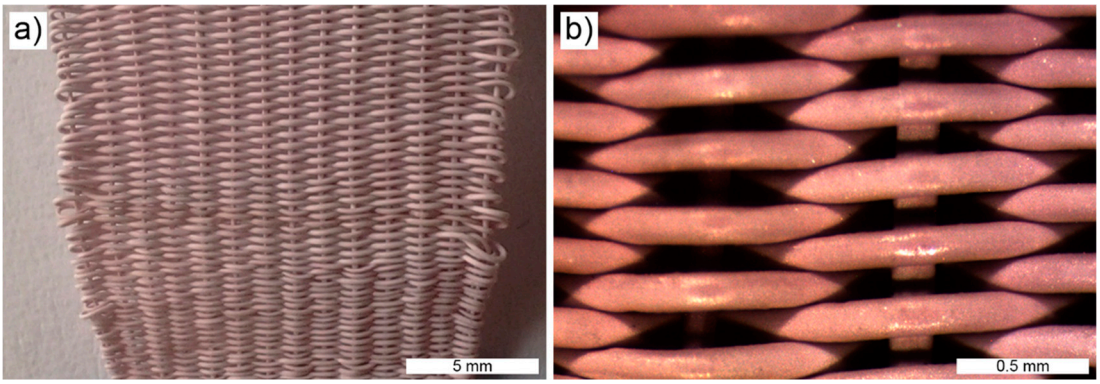

Figure 5. (**a**) Knitted fabric of gel-spun fibers of an UHMWPE–$[Fe(NH_2trz)_3](2ns)_2$ blend with ~33.3% m/m $[Fe(NH_2trz_3)](2ns)_2$ (scale bar 5 mm). (**b**) Magnification of a part of the fabric (scale bar 0.5 mm).

4. Discussion

As demonstrated above, the coordination polymer $[Fe(NH_2trz)_3](2ns)_2$ can readily be co-gel-processed with UHMWPE by extrusion to yield uniform strands. At first glance, it might be surprising that a completely non-polar polymer like UHMWPE and a highly polar polymer like $[Fe(NH_2trz)_3](2ns)_2$ can be mixed. However, the particular chemical structure of the solvent stearic acid used in the present process renders this substance to act as also a compatibilizer during processing. The amino group of NH_2trz does not coordinate to the iron(II) center and thus maintains its characteristic as a Brønsted base. On the other hand, stearic acid is a Brønsted acid. Therefore, an acid-base reaction is expected between NH_2trz and stearic acid, whereat a hydrogen cation (proton) is transferred from the carboxylic acid group of the stearic acid to the amino group of NH_2trz. Thus, $C_{18}H_{37}COO^{-}\cdot{}^{+}NH_3trz$ ion pairs are thought to form during processing, resulting in $[Fe(C_{18}H_{37}COO^{-}\cdot{}^{+}NH_3trz)_3](2ns)_2$ complexes. Hence, the long alkyl groups of the stearate envelop the polar core of the coordination polymer, rendering its external non-polar, which, in turn, makes it compatible with the non-polar UHMWPE.

The high contents of $Fe(NH_2trz)_3](2ns)_2$ in the blends rendered spin crossover visually evident by its inherent thermochromism, occurring in the usual temperature range for this coordination polymer. The corresponding spin crossover temperatures also emerge in DSC

thermograms. As mentioned in the Introduction, it is established that the spin crossover of $[Fe(NH_2trz)_3](2ns)_2$ is necessarily associated with a magnetic transition from diamagnetism to paramagnetism. The characteristic high temperature transition of $[Fe(NH_2trz)_3](2ns)_2$ is still present in the blends before as well as after drawing, and is influenced by neither UHMWPE nor by tensile drawing.

The results presented reveal that the blends combine the spin crossover properties of $[Fe(NH_2trz)_3](2ns)_2$ with the excellent mechanical properties of UHMWPE. It is highly likely that co-extrusion of UHMWPE with stearic acid as a solvent is also feasible with other polar coordination polymers, in particular when those polymers possess basic groups that are available to take up hydrogen cations from the carboxylic group of stearic acid, as discussed above for NH_2trz ligands. Noteworthy, coordination polymers can also feature a variety of other special properties [42,43], e.g., ferromagnetism, ferroelectricity, electrical conductivity, non-linear optical behavior or luminescence. Notably, as demonstrated in this work, coordination polymers themselves do not necessarily need to possess good processability, but can readily be co-processed, for instance, with UHWPE in stearic acid. Hence, it is anticipated that a variety of blends exhibiting specific properties of coordination polymers (or inorganic polymers in general) and superior mechanical properties provided by UHMWPE can be prepared by the technology presented here.

Author Contributions: Conceptualization, all authors; methodology, all authors; investigation, M.B., R.S. and I.W.; writing—original draft preparation, W.C. and R.S.; writing—review and editing, all authors; supervision, I.W. and W.C. All authors have read and agreed to the published version of the manuscript.

Funding: This research received no external funding.

Institutional Review Board Statement: Not applicable.

Informed Consent Statement: Not applicable.

Data Availability Statement: Data is contained within the article.

Conflicts of Interest: The authors declare no conflict of interest.

References

1. Dîrtu, M.M.; Neuhausen, C.; Naik, A.D.; Rotaru, A.; Spinu, L.; Garcia, Y. Insights into the Origin of Cooperative Effects in the Spin Transition of [Fe(NH2trz)3](NO3)2: The Role of Supramolecular Interactions Evidenced in the Crystal Structure of [Cu(NH2trz)3](NO3)2·H2O. *Inorg. Chem.* **2010**, *49*, 5723–5736. [CrossRef] [PubMed]
2. Grosjean, A.; Daro, N.; Kauffmann, B.; Kaiba, A.; Létard, J.-F.; Guionneau, P. The 1-D Polymeric Structure of the [Fe(NH2trz)3](NO3)2·Nh2o (With N = 2) Spin Crossover Compound Proven by Single Crystal Investigations. *Chem. Commun.* **2011**, *47*, 12382–12384. [CrossRef] [PubMed]
3. Yokoyama, T.; Murakami, Y.; Kiguchi, M.; Komatsu, T.; Kojima, N. Spin-Crossover Phase Transition of a Chain Fe(II) Complex Studied by X-Ray-Absorption Fine-Structure Spectroscopy. *Phys. Rev. B* **1998**, *58*, 14238–14244. [CrossRef]
4. Van Koningsbruggen, P.J.; Garcia, Y.; Codjovi, E.; Lapouyade, R.; Kahn, O.; Fournès, L.; Rabardel, L. Non-Classical Feii Spin-Crossover Behaviour in Polymeric Iron(II) Compounds of Formula [Fe(NH2trz)3]X2xh2o (NH2trz=4-Amino-1,2,4-Triazole; X=Derivatives of Naphthalene Sulfonate). *J. Mater. Chem.* **1997**, *7*, 2069–2075. [CrossRef]
5. Lavrenova, L.G.; Shakirova, O.G.; Ikorskii, V.N.; Varnek, V.A.; Sheludyakova, L.A.; Larionov, S.V. 1A 1⇄5 T2 Spin Transition in New Thermochromic Iron(II) Complexes with 1,2,4-Triazole and 4-Amino-1,2,4-Triazole. *Russ. J. Coord. Chem.* **2003**, *29*, 22–27. [CrossRef]
6. Voisin, H.; Aimé, C.; Vallée, A.; Bleuzen, A.; Schmutz, M.; Mosser, G.; Coradin, T.; Roux, C. Preserving the Spin Transition Properties of Iron-Triazole Coordination Polymers within Silica-Based Nanocomposites. *J. Mater. Chem. C* **2017**, *5*, 11542–11550. [CrossRef]
7. Voisin, H.; Aimé, C.; Vallée, A.; Coradin, C.; Roux, C. A Flexible Polymer-Nanoparticle Hybrid Material Containing Triazole-Based Fe(II) with Spin Crossover Properites for Magneto-Optical Applications. *Inorg. Chem. Front.* **2018**, *5*, 2140–2147. [CrossRef]
8. Bushuev, M.B.; Pishchur, D.P.; Korolkov, I.V.; Vinogradova, K.A. Prototypical Iron(II) Complex with 4-Amino-1,2,4-Triazole Reinvestigated: An Unexpected Impact of Water on Spin Transition. *Phys. Chem. Chem. Phys.* **2017**, *19*, 4056–4068. [CrossRef]
9. Vinogradova, K.A.; Pishchur, D.P.; Korolkov, I.V.; Bushuev, M.B. Magnetic Properties and Vapochromism of a Composite on the Base of an Iron(II) Spin Crossover Complex. *Inorg. Chem. Commun.* **2019**, *165*, 82–85. [CrossRef]
10. Bräunlich, I.; Sánchez-Ferrer, A.; Bauer, M.; Schepper, R.; Knüsel, P.; Dshemuchadse, J.; Mezzenga, R.; Caseri, W. Polynuclear Iron(II)–Aminotriazole Spincrossover Complexes (Polymers) in Solution. *Inorg. Chem.* **2014**, *53*, 3546–3557. [CrossRef]

11. Sánchez-Ferrer, A.; Bräunlich, I.; Ruokolainen, J.; Bauer, M.; Schepper, R.; Smith, P.; Caseri, W.; Mezzenga, R. Gels, Xerogels and Films of Polynuclear Iron(II)–Aminotriazole Spin-Crossover Polymeric Complexes. *RSC Adv.* **2014**, *4*, 60842–60852. [CrossRef]
12. Bovo, G.; Bräunlich, I.; Caseri, W.R.; Stingelin, N.; Anthopoulos, T.D.; Sandeman, K.G.; Bradley, D.D.C.; Stavrinou, P.N. Room temperature dielectric bistability in solution-processed spin crossover polymer thin films. *J. Mater. Chem. C* **2016**, *4*, 6240–6248. [CrossRef]
13. Real, J.A.; Gaspar, A.B.; Muñoz, M.C. Thermal, Pressure and Light Switchable Spin-Crossover Materials. *Dalton Trans.* **2005**, 2062–2079. [CrossRef] [PubMed]
14. Gütlich, P.; van Koningsbruggen, P.J.; Renz, F. Recent Advances of Spin Crossover Research. *Struct. Bond.* **2004**, *107*, 27–75. [CrossRef]
15. Gütlich, P.; Hauser, A.; Spiering, H. Thermisch und optisch schaltbare Eisen(II)-Komplexe. *Angew. Chem.* **1994**, *106*, 2109–2141. [CrossRef]
16. Garcia, Y.; Niel, V.; Muñoz, M.C.; Real, J.A. Spin Crossover in 1D, 2D and 3D Polymeric Fe(II) Networks. *Top. Curr. Chem.* **2004**, *233*, 229–257. [CrossRef]
17. Gütlich, P.; Goodwin, H.A. Spin Crossover—An Overall Perspective. *Top. Curr. Chem.* **2004**, *233*, 1–47. [CrossRef]
18. Barefield, E.K.; Busch, D.H.; Nelson, S.M. Iron, Cobalt, and Nickel Complexes having Anomalous Magnetic Moments. *Q. Rev. Chem. Soc.* **1968**, *22*, 457–498. [CrossRef]
19. Goodwin, H.A. Spin Transitions in Six-Coordinate Iron(II) Complexes. *Coord. Chem. Rev.* **1976**, *18*, 293–325. [CrossRef]
20. Galán Mascarós, J.R.; Aromí, G.; Darawsheh, M. Polynuclear Fe(II) Complexes: Di/trinuclear molecules and coordination netwoks. *C. R. Chim.* **2018**, *21*, 1209–1229. [CrossRef]
21. Ewald, A.H.; Martin, R.L.; Ross, I.G.; White, A.H. Anomalous behaviour at the $^6A_1$-$^2T_2$ crossover in iron (III) complexes. *Proc. R. Soc. Lond. A* **1964**, *280*, 235.
22. White, A.H.; Roper, R.; Kokot, E.; Waterman, H.; Martin, R.L. The Anomalous Paramagnetism of Iron(III) NN-Dialkyldithiocarbamates. *Aust. J. Chem.* **1964**, *17*, 294–303. [CrossRef]
23. Dîrtu, M.M.; Garcia, Y.; Nica, M.; Rotaru, A.; Linares, J.; Varret, F. Iron(II) Spin Transition 1,2,4-Triazole Chain Compounds with Novel Inorganic Fluorinated Counteranions. *Polyhedron* **2007**, *26*, 2259–2263. [CrossRef]
24. Kahn, O.; Kröber, J.; Jay, C. Spin Transition Molecular Materials for Displays and Data Recording. *Adv. Mater.* **1992**, *4*, 718–728. [CrossRef]
25. Kahn, O.; Jay Martinez, C. Spin-Transition Polymers: From Molecular Materials toward Memory Device. *Science* **1998**, *279*, 44–48. [CrossRef]
26. Kumar, K.S.; Ruben, M. Emerging Trends in Spin Crossover (SCO) Based Functional Materials and Devices. *Coord. Chem. Rev.* **2017**, *346*, 176–205. [CrossRef]
27. Molnár, G.; Rat, S.; Salmon, L.; Nicolazzi, W.; Bousseksou, A. Spin Crossover Nanomaterials: From Fundamental Concepts to Devices. *Adv. Mater.* **2018**, *30*, 17003862. [CrossRef]
28. Kuroiwa, K.; Shibata, T.; Sasaki, S.; Ohba, M.; Takahara, A.; Kunitake, T.; Kimizuka, N. Supramolecular Control of Spin-Crossover Phenomena in Lipophilic Fe(II)-1,2,4-Triazole Complexes. *J. Polym. Sci. A Polym. Chem.* **2006**, *44*, 5192–5202. [CrossRef]
29. Rubio, M.; Hernández, R.; Nogales, A.; Roig, A.; López, D. Structure of a Spin-Crossover Fe(II)–1,2,4-Triazole Polymer Complex Dispersed in an Isotactic Polystyrene Matrix. *Eur. Polym. J.* **2011**, *47*, 52–60. [CrossRef]
30. Lee, S.-W.; Lee, J.-W.; Jeong, S.-H.; Park, I.-W.; Kim, Y.-M.; Jin, J.-I. Processable Magnetic Plastics Composites—Spin Crossover of PMMA/Fe(II)-Complexes Composites. *Synth. Met.* **2004**, *142*, 243–249. [CrossRef]
31. Mallah, T.; Cavallini, M. Surfaces, Thin Films and Patterning of Spin Crossover Compounds. *C. R. Chim.* **2018**, *21*, 1270–1286. [CrossRef]
32. Salmon, L.; Catala, L. Spin-crossover Nanoparticles and Nanocomposite Materials. *C. R. Chim.* **2018**, *21*, 1230–1269. [CrossRef]
33. Enriquez-Cabrera, A.; Rapakousiou, A.; Piedrahito Bello, M.; Molnár, G.; Salmon, L.; Bousseksou, A. Spin Crossover Polymer Composites, Polymers and Related Soft Materials. *Coord. Chem. Rev.* **2020**, *419*, 213396. [CrossRef]
34. Bräunlich, I.; Lienemann, S.; Mair, C.; Smith, P.; Caseri, W. Tuning the Spin-Crossover Temperature of Polynuclear Iron(II)–Triazole Complexes in Solution by Water and Preparation of Thermochromic Fibers. *J. Mater. Sci.* **2015**, *50*, 2355–2364. [CrossRef]
35. Smith, P.; Lemstra, P.J. Ultrahigh-Strength Polyethylene Filaments by Solution Spinning/Drawing. *J. Mater. Sci.* **1980**, *15*, 505–514. [CrossRef]
36. Smith, P.; Lemstra, P.J.; Pijpers, P.L.; Kiel, A.M. Ultra-drawing of high molecular weight polyethylene cast from solution, IIL Morphology and structure. *Colloid Polym. Sci.* **1981**, *259*, 1070–1080. [CrossRef]
37. Perevedentsev, A.; Aksel, S.; Feldman, K.; Smith, P.; Stavrinou, P.N.; Bradley, D.D.C. Interplay between Solid State Microstructure and Photophysics for Poly(9,9-Dioctylfluorene) within Oriented Polyethylene Hosts. *J. Polym. Sci. B Polym. Phys.* **2015**, *53*, 22–38. [CrossRef]
38. Schaller, R.; Feldman, K.; Smith, P.; Tervoort, T.A. High-Performance Polyethylene Fibers "Al Dente": Improved Gel-Spinning of Ultrahigh Molecular Weight Polyethylene Using Vegetable Oils. *Macromolecules* **2015**, *48*, 8877–8884. [CrossRef]
39. Kaiser, W. *Kunststoffchemie für Ingenieure*, 4th ed.; Hanser: Munich, Germany, 2016; pp. 249–286. ISBN 978-3-446-44638-0.
40. Hasan, A.; Sayigh, A.A. Some Fatty Acids as Phase-Change Thermal Energy Storage Materials. *Renew. Energy* **1994**, *4*, 69–76. [CrossRef]

41. Levene, P.A.; Taylor, F.A. The Synthesis of Normal Fatty Acids from Srtearic Acid to Hexanoic Acid. *J. Biol. Chem.* **1924**, *59*, 905–921. [CrossRef]
42. Chen, C.-T.; Suslick, K.S. One-dimensional coordination polymers: Applications to material science. *Coord. Chem. Rev.* **1993**, *128*, 293–322. [CrossRef]
43. Batten, S.R.; Neville, S.N.; Turner, D.R. *Coordination Polymers*; RSC Publishing: Cambridge, UK, 2009; pp. 273–407. [CrossRef]